Combustion Chamber Fluid Dynamics and Hypergolic Gel Propellant Chemistry Simulations for Selectable Thrust Rocket Engines

Michael J. Nusca, Chiung-Chu Chen, and Michael J. McQuaid
US Army Research Laboratory, Weapons and Materials Directorate (ARL/WMD), Aberdeen Proving Ground, MD
{nusca, chiungchu.chen, mcquaid}@arl.army.mil

Abstract

This paper describes the application of high performance computing to accelerate the development of hypergolic propulsion systems for tactical missiles. Computational fluid dynamics is employed to model the chemically reacting flow within a system's combustion chamber, and computational chemistry is employed to characterize propellant physical and reactive properties. Accomplishments from the past year are presented and discussed.

1. Introduction

The US Army is developing the Impinging Stream Vortex Engine (ISVE) for tactical missile applications[1-4]. The ISVE is a hypergolic propulsion system concept, i.e., one that employs a liquid (or gelled) bipropellant combination that ignites spontaneously upon mixing at ambient temperatures and pressures. Hypergolic propulsion systems have many potential advantages over the solid propellant-based rocket motors currently employed to propel tactical missiles. Among them is active thrust control, which, increasing targeting options and range, will increase a tactical missile's lethality while reducing the vulnerability of its launch platform. Because the fuel and oxidizer are stored separately in hypergolic propulsion systems, they are also inherently insensitive to a variety of stimuli that can produce catastrophic events in solid-propellant-fueled rocket motors. The space required for conventional hypergolic system designs, however, prevents them from being integrated into airframes as small as those of tactical missiles. The ISVE concept, which facilitates the design of more compact engines, appears capable of changing this paradigm.

The primary difference between ISVE designs and conventional impinging stream engine (ISE) designs, both of which have fuel and oxidizer injection ports located in the radial wall of their combustion chamber, is the orientation at which the fuel and oxidizer are injected. In conventional ISEs, the injectors point towards the chamber's axial centerline while in the ISVE they are oriented so that (at least) initially, the fluids flow tangential to the (radial) chamber wall. The ISVE orientation forces the propellants to mix in a highly turbulent vortex region between the injector orifices and the chamber walls. There has also been some experimental evidence that centrifugal forces act to separate the heavier solid particles from the gas particles and move them toward the chamber wall. These effects have two benefits. First, they promote an increase in the mixing path length, which enables better performance to be obtained from the same-sized combustion chamber. Second, the wall temperatures are cooler than they would be in a conventional design, enabling the combustion chamber to be designed with thinner, lighter components. However, though these benefits have been observed in experimental testing that finding the combination of combustion chamber dimensions and injector orientations that maximize these benefits, and thereby engine performance, remains an issue that needs to be addressed for the technology to become viable for the intended application.

Another integral aspect of the ISVE design is the performance characteristics of the fuel and oxidizer gels. Until two years ago, the bipropellant combination employed in the experimental test program at the US Army Aviation and Missile Research, Development, and Engineering Center (AMRDEC) was monomethylhydrazine/red fuming nitric acid (MMH/RFNA). RFNA is composed primarily of nitric acid (HNO_3) and nitrogen dioxide (NO_2). However, the superior performance attributes of MMH have become outweighed by the fact that it is also acutely toxic and a suspected carcinogen. The US Army is thus funding efforts to develop an alternative (or alternatives). The two classes of compounds considered to have the best prospects for meeting desired performance objectives while having risks to human health and the environment

0-7695-3088-5/07 $25.00 © 2007 IEEE

that are acceptable are saturated, "alkyl" amines and ethanamine azides [5]. Candidates that are representative of these two classes are N,N,N'N'-Tetramethylethylene-1,2-diamine (TMEDA) and 2-Azido-N,N-dimethylethanamine (DMAZ), respectively. Representations of the molecular structure of these compounds and MMH are shown in Figure 1.

To gain insight into the relationships between design parameters and the flow physics of the engine, and thereby accelerate the development process, modeling and simulation of ISVE combustion chamber gas dynamics and engine performance (via computational fluid dynamics, [CFD]) and propellant physical properties and reactivity (via computational chemistry and material science, [CCM]) are being performed. Presented here are overviews of the CFD and the CCM technical approaches and a brief summary of results achieved over the past year.

2. CFD Modeling

CFD modeling of the ISVE is being conducted using Army Research Laboratory (ARL)-NSRG3. This program is a time-accurate CFD code that has been designed to simulate unsteady, multi-component, chemically reacting flows in various gas-dynamic applications. The latest step in its development for the ISVE[6] has been to modify it so that it can model ISVEs in which the number of individual injector pairs that are on or off can be varied. This approach to throttling the ISVE was proposed by AMRDEC to address several operational issues. The valving system enabling it is referred to as the Sliding Actuator Multi-Mode Injection Throttling Technique (SLAMMITT)[7].

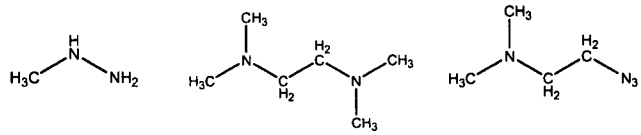

Figure 1. Hypergolic fuels

Figure 2 shows representations of the computational grids employed for CFD simulations for two ISVE designs built by AMRDEC for SLAMMITT testing. The grids employed had 180 azimuthal planes, with each having 203 cells along the chamber axis and 200 cells across the chamber diameter, for a total of about 7 million grid cells. The two engine configurations differ only in the shape of the closed (head) end of the combustion chamber. For the "flat-head" design, the combustion chamber is about 5.5 cm in diameter and the combustion chamber/nozzle combination is about 13 cm long. (The figures are not drawn to scale.) These dimensions are larger than those of previously tested ISVEs, their volume being about seven times larger than "ISVE No. 1"[3]. For the "domed-head" design, the dome corresponds to a 2:1 ellipse and the combustion chamber/nozzle combination is about 14 cm long. Fuel and oxidizer are injected into the engine through four pairs of injector orifices located around the chamber's radial wall. The azimuthal planes chosen for Figure 2 intersect with two pairs of injectors. Their locations are indicated by white bars in the chamber wall.

As a first step in examining how the combustion dynamics in these designs compare with those in smaller ISVEs fired and modeled previously (such as ISVE No. 1), the internal flowfields of these engines when run with MMH/RFNA were simulated. Figure 3 shows the pressures computed for the flat-head design as a function of time at a point at the interface between the head end and radial wall of the combustion chamber; and they are compared with values computed and measured for ISVE No. 1. (ISVE No. 1 is also a flat-head design.) Initially, the pressure in the larger engine is relatively low, but increases along with the mass flow injection rate due to the linkage between this rate and the pressure differential (i.e., the difference between the chamber and the manifold pressure). Subsequently, both the peak and steady-state pressures are larger for the larger engine.

Next, the dynamics of the domed-head design run with MMH/RFNA was simulated using the same injection schedule as that used for the large "flat-head" design and ISVE No.1. As shown in Figure 3, the chamber pressures are initially similar to the larger flat-head ISVE. However, unlike ISVE No.1 and the larger flat-head design, there is no pressure spike associated with ignition, and both the peak and steady-state pressures are less for this engine design.

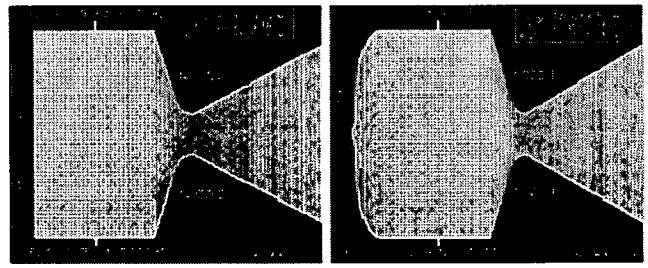

Figure 2. Computational grids for SLAMMITT ISVE designs. Shown is a single azimuthal plane containing two pairs of opposed injectors. (For clarity, not all cells are plotted).

Figure 4 compares the computed pressure contours (range 0 to 2 kpsia: blue to red color) for the two new designs with selected velocity vectors superimposed. For a time close to steady operation (0.440 seconds), pressures are high near the injectors and within the flow stagnation

region near the head-end of the chamber. It can be observed that the domed-head mitigates the formation of high pressures in this region, and on this basis, AMRDEC decided to conduct all future testing of the SLAMMITT concept with the domed-head design.

Finally, the dynamics of the SLAMMITT-equipped domed-head design was simulated using a propellant injection schedule derived from an experimental test. In this case, the MMH and RFNA were injected simultaneously using one to four pairs of injectors. The pressure histories generated by the simulation are plotted in Figure 5. Engine thrust was also recorded during the SLAMMITT test. (The measured data[7] is not reproduced in this paper.) Measured thrust levels were about 100 lb_f during both of the "low thrust" operations and about 400 lb_f for the "high thrust" operation. The computed thrust levels (see Figure 5, "Thrust Method 1") are slightly higher than the measured data, with the largest discrepancy for the second "low thrust" operation. The "top hat" shape to the thrust curve indicates that the engine responds rapidly to throttling.

3. Computational Chemistry

The steps being proposed for the chemical kinetics mechanisms for TMEDA/RFNA and DMAZ/RFNA systems follow from those in ARL's mechanism for MMH/RFNA[8 (and references therein)]. That is, various (exothermic) complexation reactions and addition reactions provide the energy needed to promulgate H-atom abstraction reactions of the fuel (parent) and its dehydrogenated daughters. The daughters further decompose via β-scission reactions, and radicals from those reactions are oxidized to complete the combustion process. The development of TMEDA/RFNA and DMAZ/RFNA mechanisms is, however, a much bigger challenge than the MMH/RFNA mechanism was. MMH's preeminence as a hypergol had led to many previous studies of its combustion chemistry, and a large part of the mechanism could be constructed from them. ARL needed only to supplement that information, refining parameters for certain reaction steps and adding a small set of additional reactions so that simulations more closely approximated the behavior of experimentally characterized systems. Very little has been reported on the combustion of amines (in general) let alone TMEDA or DMAZ. Therefore, the mechanisms for them have had to be built essentially from scratch. An additional difficulty is that TMEDA and DMAZ are much larger molecules than MMH: eight heavy (non-hydrogen) atoms vs. three heavy atoms. Thus there are many more potential pathways for their decomposition to take. A full, detailed mechanism that is to be the basis for a "reduced" mechanism that will be employed for the CFD modeling effort was constructed this year. It contains over 1,000 reaction steps involving over 400 species. This paper summarizes results for the mechanisms of reaction for one pair of reactants: CH_3CH_2·and NO_2.

Thermochemical parameters for the stationary points of identified reaction paths are derived from calculations based on various levels of *ab initio* and density functional theories. Molecular structures and frequencies are calculated via B3LYP/6-31G(d,p) and MPWB1K/6-31+G(d,p) models. Refined energy characterizations are then obtained with B3LYP/6-311+G(2df,p), G3, G3MP2 and CBS-Q models. CCSD(T) calculations with relatively large basis sets are also performed for (small) molecules for which they are practical. All QM calculations reported here were performed with the Gaussian 03 suite of codes[9]. Entropies and heat capacities are calculated from methods of (macro-canonical) statistical mechanics using vibration frequencies, moments of inertia, and internal rotation parameter data obtained from the calculations and literature where available.

For reactions where the thermodynamic properties of a transition state (TS) need to be calculated, the value is not simply the total energy difference between reactant(s) and transition state. Rather it is the average of two values: $\Delta H_{R,\,calc.}$ and $\Delta H_{P',\,calc.}$; where $\Delta H_{R,\,calc.}$ is the difference between the calculated energy of the TS and reactant(s) and $\Delta H_{P',\,calc.}$ is the difference between the calculated energy of the TS and product(s) plus ΔH_{rxn} ($\Delta H^{\circ}_{f\ product(s)} - \Delta H^{\circ}_{f\ reactant(s)}$). A three-parameter equation for k_∞: $k_\infty = A_\infty(T)^{\Delta n}\exp(-E_a/RT)$; is then fit to the data over a temperature range from 298 to 3,000K. Entropy differences between reactants and the TS are employed as input to canonical transition state theory to determine the pre-exponential factor (A). High-pressure limit pre-exponential factors for recombination reactions are obtained from the literature and from trends in homologous series of reactions. Activation energies are calculated from analysis of Evans Polanyi relationships for abstractions plus evaluations of ring strain energy, and from analogy to similar reactions with known energies.

Unimolecular dissociation and isomerization reactions of the chemically activated and stabilized adducts resulting from addition or recombination reactions are analyzed by first constructing potential energy diagrams for the reaction system. Kinetics parameters for unimolecular and bimolecular (chemical activation) reactions are then calculated using multi-frequency QRRK analysis for $k(E)$[10–12] with the steady state assumption for the energized adduct(s). The master equation analysis discussed by Gilbert is used for fall-off[13–15].

Potential energy diagrams for paths that the reaction of CH_3CH_2·with NO_2 can take are shown in Figure 6. The

addition of NO_2 to CH_3CH_2· forms chemically activated $CH_3CH_2NO_2$* or CH_3CH_2ONO* adducts that have well-depths of approximately 60 kcal/mol. The reaction channels of the $CH_3CH_2NO_2$* adduct include: (1) dissociation back to reactants, (2) stabilization to $CH_3CH_2NO_2$, (3) isomerization via TS2 to CH_3CH_2ONO, and (4) the formation of *trans*-HONO + C_2H_4 via TS1. The C_2H_5ONO* adduct can: (1) dissociate back to reactants, (2) form *cis*-HONO + C_2H_4 via four- and six-member ring transition states (TS3 and TS4), (3) form HNO_2 + C_2H_4 via a five- member ring (TS5), (4) stabilize to CH_3CH_2ONO, (5) isomerize to $CH_3CH_2NO_2$, and (6) dissociate to CH_3CH_2O· and NO. High-pressure rate constants (k_∞) calculated using canonical TST along with B3LYP/6-31G(d,p)-determined entropies and CBS-Q//B3DP model energies are shown in Table 1.

QRRK/Master Equation-calculated rate constants for forward reactions at 75 atm as a function of temperature are illustrated in Figure 7. CH_3CH_2O-NO bond fission to form the CH_3CH_2O· oxy radical is the dominant reaction channel because the CH_3CH_2O-NO bond is substantially (ca. 20 kcal/mol) weaker than the CH_3CH_2-ONO bond. The stabilization rate of the CH_3CH_2ONO adduct significantly increases with increase in pressure. Similar analyses have been performed for other reactions relevant to the mechanism and will be published elsewhere.

Table 1. Parameters for high-pressure limit rate constants (k_∞) from QRRK calculations: CH_3CH_2· + NO_2 → products

	A (s^{-1} or cm^3/mol·s)	*n*	E_a (kcal/mol)
CH_3CH_2· + NO_2 → $CH_3CH_2NO_2$	6.8×10^{12}	0.00	0.0
$CH_3CH_2NO_2$ → *trans*-HONO + C_2H_4 (via TS1)	6.5×10^{19}	1.05	45.6
$CH_3CH_2NO_2$ → CH_3CH_2ONO (via TS2)	3.0×10^{11}	0.71	61.8
CH_3CH_2· + NO_2 → CH_3CH_2NO	2.0×10^{13}	0.00	0.0
CH_3CH_2ONO → *cis*-HONO + C_2H_4 (via TS3)	1.2×10^{11}	1.17	64.5
CH_3CH_2ONO → *cis*-HONO + C_2H_4 (via TS4)	9.8×10^{09}	0.94	56.1
CH_3CH_2ONO → HNO_2 + C_2H_4 (via TS5)	2.2×10^{10}	0.78	50.7
CH_3CH_2ONO → *trans*-HONO + C_2H_4 (via TS6)	3.2×10^{10}	1.16	66.4
CH_3CH_2ONO → CH_3CH_2O· + NO	2.7×10^{17}	0.00	41.8

4. Summary of Accomplishments and HPC Resources Utilized

The application of modern computational fluid dynamics to the chemically reacting flow within the ISVE has yielded visualizations of combustion dynamics within new ISVEs designed to test the SLAMMITT concept. The simulations have had a strong influence on the course of the experimental testing program at AMRDEC.

A full, multi-step, chemical kinetics reaction mechanism having over 1,000 reaction steps and involving over 400 species has been developed to model TMEDA/RFNA systems. (It will be "reduced" for use with the CFD model of the ISVE.)

These accomplishments have been achieved at the expense of about 90,000 hours on a Cray X1e and about 94,000 hours on the Aeronautical Systems Center (ASC) SGI O3K. The ARL-NSRG3 CFD code was run on the Cray while the CCM codes were executed on the ASC SGI (HPC11). It is anticipated that the balance of the Challenge project's HPC hours will be used in the next few months as further simulations are performed.

Acknowledgements

The Department of Defense (DoD) HPC Modernization Program supported this project by supplying supercomputer time under the Computing Challenge Project C2N. This computer time was made available at the DoD Major Shared Resources Centers at ASC, and the Distributed Center at the Army High Performance Computing Research Center-NetworkCS. Mr. R.S. Michaels and Ms. L. Felton from AMRDEC provided helpful information concerning the ISVE and its propellants. Dr. W. Anderson (ARL) formulated the initial "full" MMH/RFNA chemical reaction mechanism. Dr. A. Kotlar (ARL) formulated the "reduced" MMHRFNA chemical reaction mechanisms used with the CFD code. Prof. Y. Ishikawa (University of Puerto Rico) has helped conduct QM-based studies.

References

1. Wilson, B F., and Connaughton, J.W., "Investigation of a Unique Design Engine Assembly." *Proceedings of the 3rd AIAA Propulsion Joint Specialist Conference*, Washington, DC, 17–21 July, 1967.

2. Michaels, R.S. and B.F. Wilson, "The Low L/D Vortex Engine for Gel Propulsion." *Proceedings of the 1995 JANNAF Gel Propulsion Technology Symposium*, CPIA Pub. 627, pp. 9–16, 1995.

3. Nusca, M.J. and R.S. Michaels, "Development of a Computational Model for the Army's Impinging Stream Vortex Engine." *Proceedings of the 1st JANNAF Liquid Propellant*

Subcommittee Meeting, Las Vegas, NV, CPIA Publication JSC CD-33, 2004.
4. Nusca, M.J. and M.J. McQuaid, "Combustion Chamber Fluid Dynamics and Hypergolic Gel Propellant Chemistry Simulations for Selectable Thrust Rocket Engines." *Proceedings of the HPCMP Users Groups Conference, Denver, CO*, IEEE Computer Society, 2006.
5. McQuaid, M.J., "Notional Hydrazine-Alternative Hypergols: Design Considerations, Computationally-Based Property Determinations, and Acquisition Possibilities." *ARL-TR-3694*, Aberdeen Proving Ground, MD, 2006.
6. Nusca, M.J., N.P. Mathis, and R.S Michaels, "Computational Modeling of the Army's Impinging Stream Vortex Engine Including an Injection Throttling System." *Proceedings of the 3rd JANNAF Liquid Propulsion Subcommittee Meeting*, CPIA Publication (in press), 2007.
7. Mathis, N.P., T.W. Turner, R.S. Michaels, and J.H. Arszman, "Development and Demonstration of Vortex Engine Throttling Techniques." *Proceedings of the 3rd JANNAF Liquid Propulsion Subcommittee Meeting*, CPIA Publication (in press), 2007.
8. Ishikawa, Y. and M.J. McQuaid, "H-Atom Abstraction from CH_3NHNH_2 by NO_2: CCSD(T)/ 6-311++G(3df,2p)//MPWB1K/6-31+G(d,p) and CCSD(T)/6-311+G(2df,p)//CCSD/6-31+G(d,p) Calculations." *J. Phys. Chem. A*, 110, pp. 6129–6138, 2006.
9. Frisch, M.J., et al., *Gaussian 03, Revision B.05*, Gaussian, Inc., Pittsburgh PA, 2003.
10. Westmoreland, P.R., J.B. Howard, J. P. Longwell, A.M. Dean, AICHE Annual Meeting, 32, 1971, 1986.
11. Westmoreland, P.R. *Combust. Sci. and Tech.*, 82, 1515, 1992.
12. Dean, A.M. and P.R. Westmoreland, *Int. J. Chem. Kinet.* 19, 207, 1987.
13. Gilbert, R.G. and S.C. Smith, *Theory of Unimolecular and Recombination Reactions*, Oxford Press, 1990.
14. Chang, A.Y., J.W. Bozzelli, and A.M. Dean, *Z. J. Phys. Chem. A* , 104, 1533, 2000.
15. Gilbert, R.G. and K. Luther, and Troe, *J. Ber. Bunsenges. Phys. Chem.*, 87, 164, 1983.

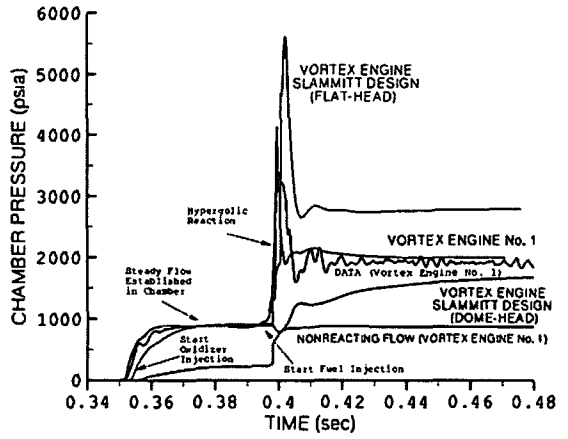

Figure 3. Comparison of computed chamber pressures for SLAMMITT ISVE flat-head and domed-head designs with measured values for ISVE No.1

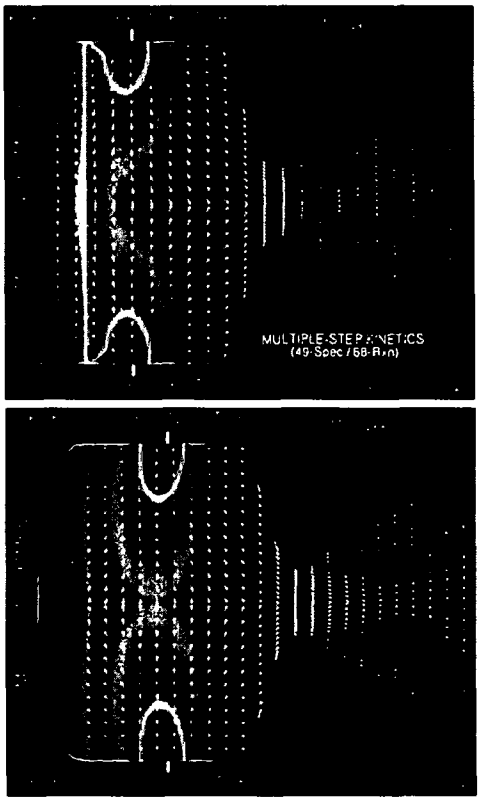

Figure 4. Contours of pressure and selected velocity vectors at steady state for SLAMMITT ISVEs: (A) Flat-head design; (B) Domed-head design

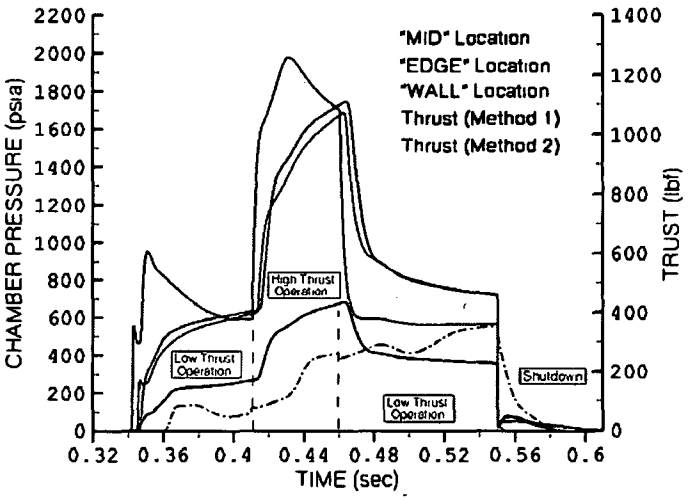

Figure 5. Computed chamber pressures and thrust for the domed-head SLAMMITT ISVE design

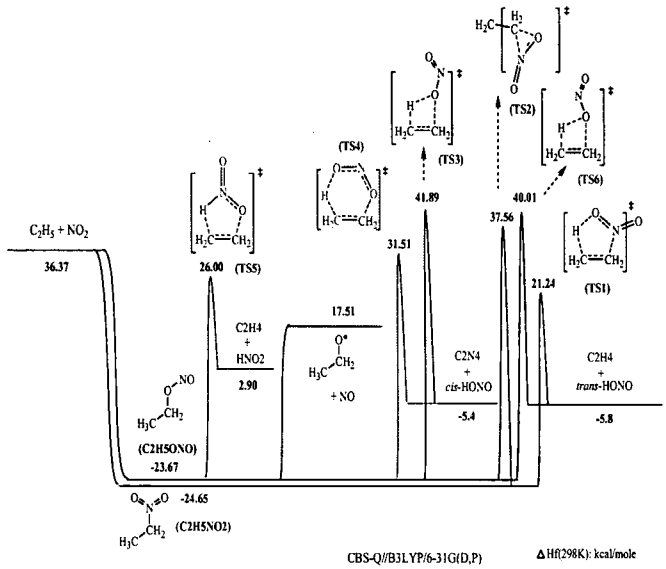

Figure 6. Potential energy diagrams for CH_3CH_2·+ NO_2 system reaction paths

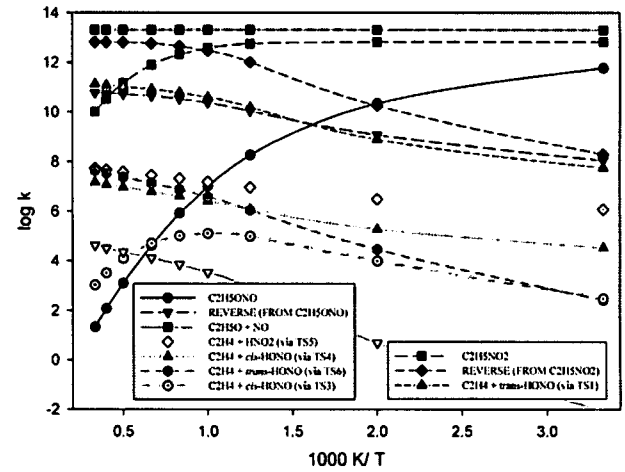

Figure 7. QRRK rates for the CH_3CH_2·+ NO_2 system as a function of temperature at 75 atm